

# MULTISPECTRAL IMAGING SYSTEMS USING ACOUSTO-OPTIC TUNABLE FILTER

Li-Jen Cheng, Tien-Hsin Chao, Mack Dowdy,  
Clayton Labaw, Colin Mahoney, and George Reyes  
Jet Propulsion Laboratory, California Institute of Technology  
Pasadena, CA 91109

Ken Bergmen  
Amy Space Technology and Research Office  
Ft. Belvoir, VA 22060

## ABSTRACT

This paper discusses recent activities of Jet Propulsion Laboratory (JPL) in the development of a new type of remote sensing multispectral imaging instruments using acousto-optic tunable filter (AOTF) as programmable bandpass filter. This remote sensor provides real-time operation; observational flexibility; measurements of spectral, spatial, and polarization information using a single instrument; and compact, solid state structure without moving parts. An AOTF multi spectral imaging prototype system for outdoor field experiments was designed and assembled. Some preliminary experimental results are reported. The field system will be used to investigate spectral and polarization signatures of natural and man-made objects for evaluation of the technology feasibility for remote sensing applications. In addition, an airborne prototype instrument is currently under development.

## 1. INTRODUCTION

The multispectral imaging system using acousto-optic tunable filter (AOTF) provides unique observation capabilities. It can observe a scene as a function of spatial, spectral, polarization, and time coordinates, namely, all the information parameters available through the electromagnetic wave medium. Basically, AOTF is a high resolution, fast tunable spectral bandpass filter using the diffraction of incident light beam at a moving grating produced by an acoustic wave in a birefringent crystal. An AOTF instrument is capable of taking two orthogonally polarized images at a desired wavelength at one time. The selection of operation wavelength is done by tuning the frequency of a RF power applying the transducer on the crystal. Therefore, the filter can operate in a sequential, random (wavelength hopping), or multiple wavelength mode, providing a unique operation flexibility.

AOTFs can provide high spectral resolution ( $\lambda/\Delta\lambda$ ) of 10<sup>2</sup>-10<sup>4</sup>. This high resolution capability gives opportunities of characterizing materials through the measurement of its reflection, absorption, or emission spectra.

The operation wavelength range of an AOTF depends on the birefringent crystal used. For example, TeO<sub>2</sub> crystal is a common birefringent material transparent in a wavelength range of 0.4-5 microns. AOTF can operate in any wavelength within this transparent range, but each AOTF can only operate within a wavelength range in one octave, because of the transducer operation frequency limitation. Other attractive features of using an AOTF include large throughput; compact, rugged and lightweight construction; and all solid-state structure without moving parts.

In the past, we built two AOTF imaging spectrometer breadboard systems covering visible to short-wavelength infrared wavelength ranges and demonstrated successfully capabilities to identify minerals and map content distributions; characterize botanical objects; and measure polarization signatures.<sup>1-4</sup> In addition, we demonstrated the use of an optical

fiber bundle as image transfer vehicle in the AOTF system with the objective to develop an AOTF system with a flexible observation head in future.

In this paper, we discuss recent progress at JPL in the development of AOTF multispectral imaging systems for remote sensing applications. The work includes design, assembly, and tests of an AOTF polarimetric multispectral imaging prototype system for outdoor field remote sensing experiments as well as preliminary design of an airborne prototype system. The objective of this task is to evaluate AOTF multispectral imaging technology for Army space tactical applications and remote sensing in general.

## 2. GENERAL DESCRIPTION OF AOTF

Harris and Wallace<sup>5</sup> proposed the first AOTF utilizing collinear acousto-optic interactions. Later, Chang<sup>6</sup> invented the noncollinear AOTF. The noncollinear AOTF has large angular aperture and is suitable for multispectral imaging applications.

Figure 1 shows the schematic of a noncollinear AOTF. It consists of a birefringent crystal to which one or several piezoelectric transducers are bonded. When a RF signal is applied, the transducer generates acoustic waves launching into the crystal. The propagating acoustic waves produce a periodic modulation of index of refraction. This provides a moving phase grating that diffracts portions of an incident light beam. For a fixed acoustic frequency and sufficiently long interaction length, only a narrow band of optical frequencies can satisfy the phase-matching condition and be diffracted. As the RF frequency changes, the center of optical bandpass changes accordingly, because the phase-matching condition must be satisfied.

The above description of an acousto-optic spectral filtering mechanism applies to both an isotropic medium and to a birefringent crystal. However, in an isotropic medium the filtering action is extremely sensitive to the angle of the light incidence and is thus usable only for collimated light.

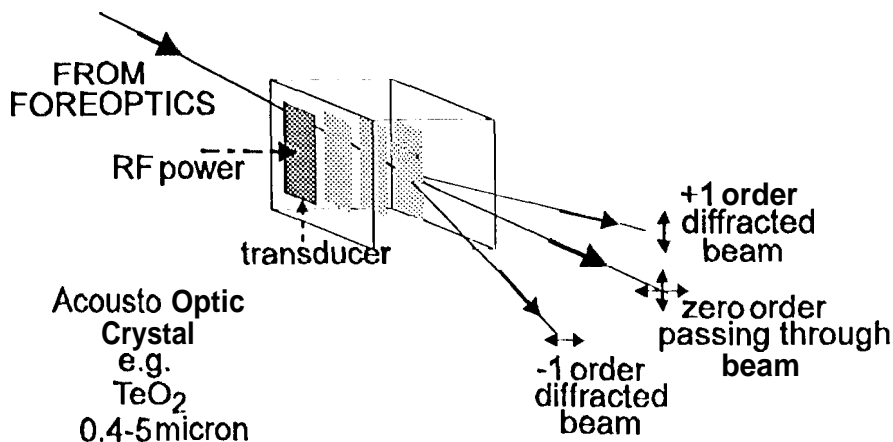
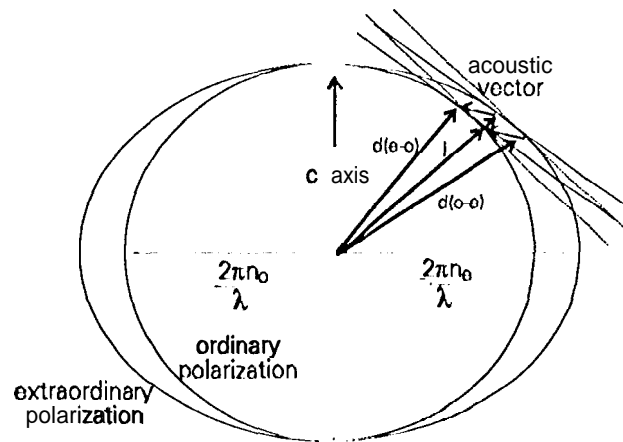


Figure 1. Schematic of a non-collinear AOTF. The filter diffracts an incoming beam into two orthogonally polarized beams at a selected wavelength.



$i$  = incident beam       $d(o-o)$  = diffracted beam from ordinary wave to extraordinary wave       $d(e-o)$  = diffracted beam from extra-ordinary wave to ordinary wave

Figure 2. Wave vector diagram (k-space) for noncollinear AOTF

in an anisotropic medium such as a uniaxial crystal, there are two different refraction index surfaces: one for the ordinarily polarized light and the other for the extraordinarily polarized light. In this case, the acoustic wave may diffract an incident polarized light into the orthogonal polarization. For this birefringent diffraction it is possible to satisfy the phase-matching condition for incident light having a range of incidence angles. Figure 2 gives a wave vector diagram to illustrate the basic concept for acousto-optic diffraction in a uniaxial crystal. The acoustic wavevector is chosen so that the tangents to the incident and diffracted light wavevector surfaces are parallel. When this parallel tangent condition is met, the acousto-optic diffraction becomes relatively insensitive to the angle of light incidence, a process that is referred to as noncritical phase-matching. If the incident beam is unpolarized, there will be two orthogonally polarized diffracted beams exiting at the opposite sides of the undiffracted beam, as illustrated in Figure 1. This provides opportunities to measure polarization of incident light.

Tellurium oxide ( $\text{TeO}_2$ ) is the preferred acousto-optic material for the visible, near-infrared and mid-infrared spectral regions (0.4-5 microns) because of the availability of high-quality crystals.<sup>7</sup> There are several other materials that can be used in the far-infrared range (to 11 microns).<sup>8</sup> Among them,  $\text{Tl}_3\text{AsSe}_3$  is the one that is commercially available. For ultraviolet wavelengths, quartz is a good candidate. This work uses AOTFs of  $\text{TeO}_2$ .

### 3. OUTDOOR FIELD PROTOTYPE SYSTEM

#### 3.1 System Description

The system contains an optical subsystem, two integrating CCD cameras, a RF generator and a power amplifier, a 386 PC compatible computer for control and data acquisition, and monitors. The unique part of the system is the optical configuration which is discussed briefly in the following paragraphs.

AOTF imposes two restrictions on optical system design. The first is the small field of view of the filter, about 6-10 degrees in full field of view, depending on design. The second is the limitation of AOTF aperture size due to fabrication technology limitation and attenuation of acoustic wave in AO crystal. In general, any observation system shall have high collection efficiency. This requirement is specially important for the AOTF system, because it is a high-resolution instrument. With these restrictions and application requirements in mind, we designed an optical system which utilizes maximum capabilities provided by AOTF.

Figure 3 gives an illustration of the optical configuration used in the newly-assembled AOTF multispectral imaging system for outdoor observations. It contains a 3 inch aperture, zoom telelens set with variable focal length of 80-120 mm as the objective lens; an aperture locating at the objective lens image plane for allowing only photons from the desired scene to pass through; a collimating lens ( $f=40\text{mm}$ ) to create an intermediate pupil plane whose cross section is comparable with that of AOTF; an AOTF locating at the pupil plane, a field lens to create adequate beam diversion for imaging at the cameras; and two cameras for recording two polarized images separately. The distances between the field lens and cameras are relatively long, because of the small diffraction angles in the AOTF used. This distance will be substantially reduced after an adequate AOTF becomes available.

According to geometric optics, the ratio of  $f_1/f_2$  is equal to  $\alpha_2/\alpha_1$  and  $d_1/d_2$ , where  $f_1$  and  $f_2$  are focal lengths of objective lens and collimating length,  $\alpha_1$  and  $\alpha_2$  are acceptance angles of the system and AOTF, and  $d_1$  and  $d_2$  are apertures for objective lens and AOTF, respectively. These relationships provide a guide to design an AOTF system. In our system, we use off-the-shelf optical components with some compromise.  $\alpha_2$  and  $d_2$  of the AOTF used in the system are  $7^\circ$  and 10 mm, respectively. The  $f_1/f_2$  ratio of our system varies within the range of 2-5, because a zoom lens set is used. Therefore the system field of view can vary within a range of 1.4-3.5 degrees. The field of view in this range is adequate for outdoor observations of natural and man-made objects.

Figure 4 gives a photo of the ground system without cover. Two Photometrics Star-1 integrating silicon CCD camera are used as shown in the photo. The time integrating capability provides opportunities to observe objects under a wide range of light conditions. This capability is needed for the evaluation of the AOTF multispectral imaging technology.

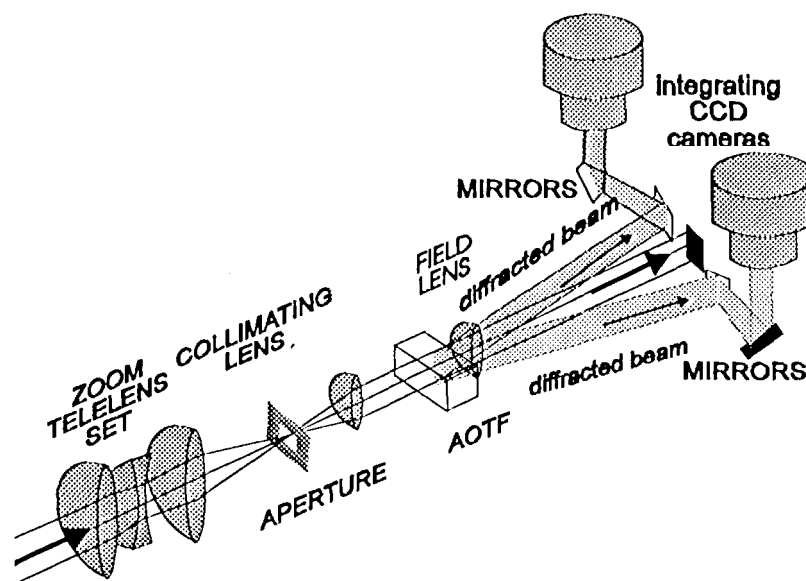


Figure 3. Schematic diagram of the ground system optical configuration.

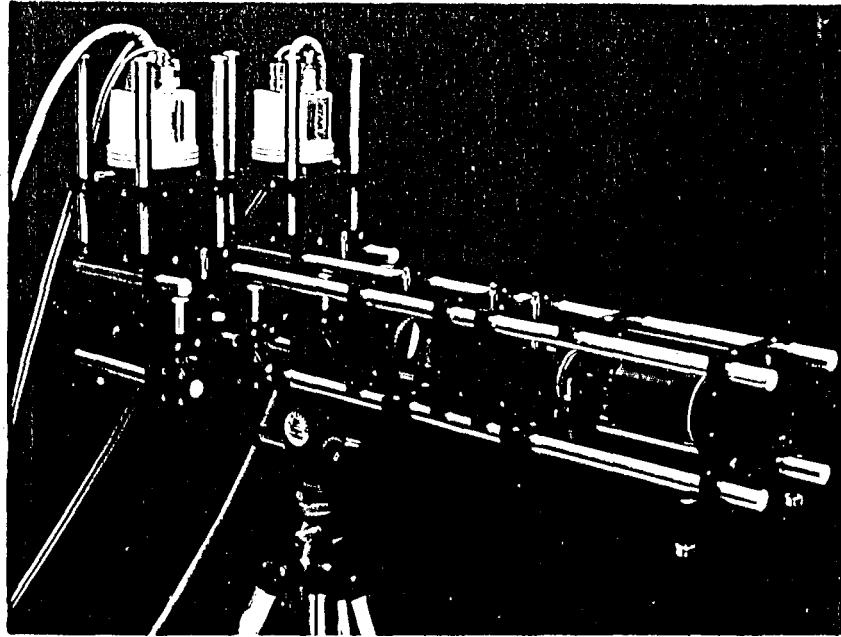


Figure 4. Photo of the ground system without the cover.

### 3.2 Preliminary Test Results

#### 3.2.1 Reflective Spectra of Bastnaesite Rock

The experiment purpose is to test system capability of measuring spectral properties of an object. A bastnaesite rock sample from the Mountain Pass, California, was used. This mineral contains neodymium and samarium fluorocarbonate in a silica matrix. During the measurement, the rock was illuminated by a sunlamp. A small compressed  $\text{II Al}_2\text{O}_3$  powder disk was placed on the rock as reference reflector whose scattering reflectance is unity over the wavelength range of interest. Under this condition, the system has the ability to compute the reflectivity and output the reflectance spectrum directly. Figure 5 gives two measured reflectance spectra of a selected portion of the rock at two polarization directions. The measured spectra for both polarization directions are practically the same, as expected from the rock sample, because the reflection from the rock surface do not have any polarization effect. The figure also gives a reflectance spectrum of a similar sample using a conventional high-resolution Beckman spectrometer for comparison.<sup>9</sup> This similarity among the three spectra illustrates the capability of the system for measuring accurately reflectance spectra, including polarization.

#### 3.2.2 Outdoor Spectral Observations

We did the first outdoor test in a heavily cloudy day with occasional rains. The light condition was very poor. Because of using the integrating cameras, we were able to take reasonable good spectral photographs. Figure 6 gives two images of a red-brown-colored roof house and surroundings located about one Km away from the system. One was taken at 770 nm at which the chlorophyll reflection from vegetation was strong. The other was taken at 630 nm (red) and vegetation reflection was weak. There are a number of interesting features appearing clearly in comparison of these two photos. For example, the red roof was very bright in the 630 nm picture, but dark in the 770nm picture. A street light fixture above the house was clearly observable in the 630 nm picture, but not in the 770 nm picture. This could be due to the fact that the background tree leaves became as bright as the light fixture at 770 nm. Furthermore, under this condition, electrical power lines above the house becomes observable in the infrared picture, but not in the 630 nm picture. In the lower part of the 630 nm picture, there is a black line, due to a power line located at some distance away from the front of the house. But this black line disappears in the 770 nm picture. This disappearance could be due to spectral properties of the coating material on power line.

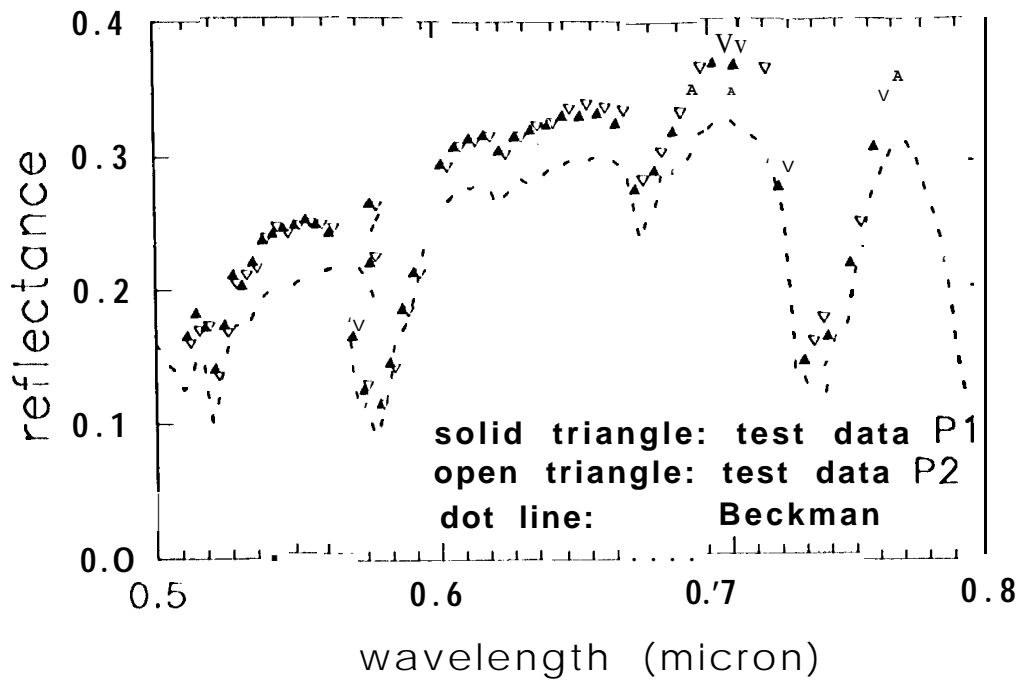


Figure 5. Measured reflectivity spectra of a Bastnacsite rock at two polarization orientations in comparison with data taken from a similar rock using a conventional Beckman spectrometer.

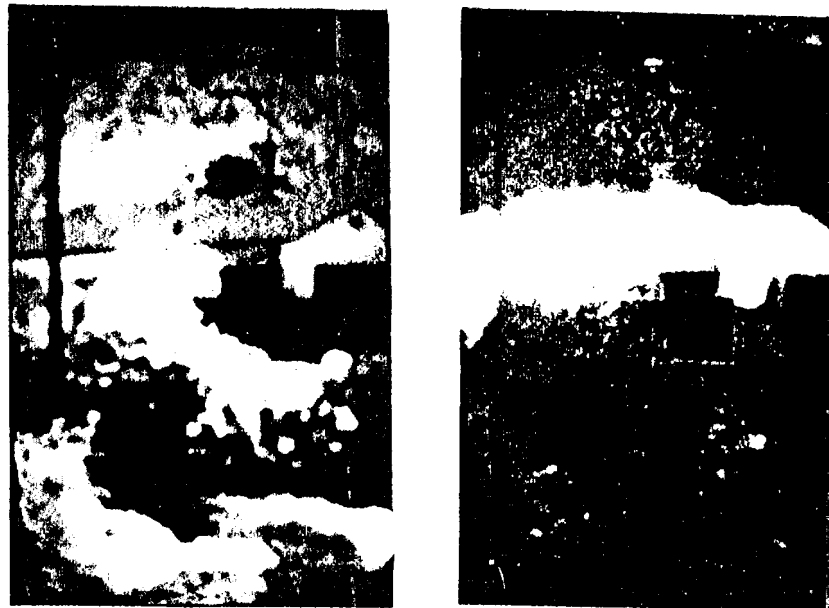


Figure 6 AOTF Images taken using the ground system at wavelengths of 630 nm (right) and 770 nm (left).

The above stated observations illustrates the discriminating capability of multispectral imaging. More experiments are in progress with the objectives to learn effective ways of using the multispectral imaging instrument, to evaluate the technology feasibility, and to collect valuable signature data.

#### 4. BRIEF DESCRIPTION OF AIRBORNE PROTOTYPE SYSTEM

We started to develop an AOTF multispectral imaging prototype system for airborne technology demonstration experiment. The experiment will be carried out from a platform in a jet airplane. A tentative specification list of the airborne system was created by a joint effort of Aerospace Corporation, JPL, Massachusetts Institute of Technology/Lincoln Laboratory, U.S. Army Intelligence Center and School, and U.S. Army Space Technology and Research Office. The tentative specifications are briefly stated in the following:

1. A NASA-Lewis Lear Jet will be the experiment platform at an altitude about 30000 ft.
2. Sample rate of the system is 60 frames per second. The time required for observing a target is one second at minimum.
3. Spatial resolution is 1-2 meters.
4. Effective target cross section is equal or larger than  $4 \text{ m}^2$ .
5. Si CCD focal plane arrays of  $64 \times 256$  pixels available from MIT/Lincoln Laboratory will be used. The arrays will operate at the airplane cabin temperature without any cooling if the signal-to-noise ratio is acceptable.
6. Detected signals will be in 12 bit format. This provides a dynamic range of 4096.
7. The instrument will be on NASA-Ames Gyro Stabilized Helistat for observation and target tracking. There will be two tracking cameras, one narrow field-of-view camera to be boresighted through AOTF zeroth order image and one wide-angle searching and pointing camera.

Functionally, the system contains three subsystems: optical, signal acquisition and storage, and target tracking. In addition, a mechanical structure holding the instrument will be designed and fabricated. At present, we have completed preliminary designs on mechanical mounting, stress analysis, optical configuration, tracking mechanism, and electronic apparatus. The results indicate that adequate performance of the airborne system is expected. We plan to complete the instrument and start experiments in the summer of 1994.

#### 5. ACKNOWLEDGMENTS

The work described in this paper was performed by the Center for Space Microelectronics Technology, Jet Propulsion Laboratory, California Institute of Technology, under a contract with the National Aeronautics and Space Administration, and was sponsored by the Army Space Technology and Research Office and the National Aeronautics and Space Administration. We would like to acknowledge contributions of the team of experts from Aerospace Corporation, Jet Propulsion Laboratory, Massachusetts Institute of Technology/Lincoln Laboratory, U.S. Army Intelligence Center and School, and U.S. Army Space Technology and Research Office who created the tentative specifications for the airborne system.

#### 6. REFERENCES

1. T.H. Chao, J. Yu, L.J. Cheng, J. Lambert, "Optical information Processing Systems and Architectures I", SPIE Proceedings, Vol. 1347, p.655 (1990).
2. J. Yu, T.H. Chao, and L.J. Cheng, "Optical information Processing Systems and Architectures II", SPIE Proceedings, Vol. 1347, p.664 (1990).

3. T. H. Chao, J. Yu, G. Reyes, D. Rider and L. J. Cheng, "Acousto-Optic Tunable imaging Spectrometers" Proceedings of 1991 International Geoscience and Remote Sensing Symposium, Helsinki, Espoo, FINLAND, June, 1991 (IEEE 91(312971-0), p. 585.
4. L. J. Cheng, T. H. Chao, and G. Reyes, "Acousto-Optic Tunable Filter Multispectral imaging System" AIAA Space Programs and Technologies Conference, March 24-27, 1992, paper no, 92-1439
5. S.E. Harris and R.W. Wallace, "Acousto-Optic Tunable Filter", J. Opt. Soc. Am. 59, 774 (1969).
6. I.C. Chang, "Nonlinear Acousto-Optic Filter with Large Angular Aperture", Appl. Phys. 1AM, & 370(1974).
7. I.C. Chang, "Acousto-Optic Tunable Filters", Opt. Eng. 20, 824 (1981).
8. P. Katzka, SPIE vol. 753, "Acousto-Optic and Magneto-Optic Devices and Applications" (1987), p. 22.
9. R.O. Green, "Retrieval of Reflectance from Calibrated Radiance Imagery Measured by the Airborne Visible/Infrared imaging Spectrometer (AVIRIS) for Lithological Mapping of the Clark Mountains, California", in "Proceedings of the Second Airborne Visible/Infrared imaging Spectrometer (AVIRIS) Workshop" edited by R.O. Green, [J], Publication 90-54), p.167 (1990).